Full text open access online (Since 2001)

PRINT: ISSN 0972-3757 ONLINE: ISSN 2456-6330
Int J Hum Genet, 24(1): 18-28 (2023)
DOI: 10.31901/24566322.2023/24.01.807

MiR-155 Promotes Ischemic Stroke by Inhibiting mTOR Protein Expression

Wenli Huang, Quanlong Hong, Huimin Wang, Shujie Gong, Zhihua Zhu and Zhuquan Hong*

Department of Neurology, Quanzhou First Hospital Affiliated to Fujian Medical University, Quanzhou, Fujian, China, 362000

KEYWORDS BV2 Cell. Ischemic Stroke. miR-155. mTOR Protein. Oxygen-Glucose Deprivation

ABSTRACT The researchers aimed to determine the serum miR-155 expression in ischemic stroke (IS) patients. Serum samples were obtained to detect miR-155 expression. National Institute of Health Stroke Scale (NIHSS) was applied to assess neurological deficits. An oxygen-glucose deprivation (OGD) model of mouse microglial BV2 cells was established. Transfection of BV2 cells with miR-155-mimic/mimic-negative control (NC) or miR-155-inhibitor/inhibitor-NC was conducted. Markedly elevated miR-155 expression in serum of IS patients was detected in comparison with that in healthy individuals ($P<0.001$). NIHSS score declined progressively on 1st, 7th and 14th days after onset ($P<0.005$). The survival rate of BV2 cells after OGD treatment decreased evidently ($P<0.001$). Moreover, miR-155 expression was significantly reduced, but the protein expression of mTOR increased in OGD group ($P<0.05$). The downregulation of miR-155 facilitated mTOR mRNA and protein expressions ($P<0.005$). Elevated miR-155 is associated with the pathogenesis of IS and negatively correlated with prognosis. MiR-155 suppresses mTOR protein expression in mouse microglial BV2 cells and facilitates OGD-induced stress response.

INTRODUCTION

Ischemic stroke (IS) ranks second in mortality and forefront in disability (Gervois and Lambrichts 2019). Patients who suffer from IS constitute about 80 percent of all stroke individuals (Charbonnier et al. 2020). The incidence rate of IS is 18.3 percent, prominently higher than that of hemorrhagic stroke (8.2%) (Feigin et al. 2018). Attributing to the high morbidity, disability, recurrence and mortality rates of IS, making efforts to elucidate the mechanisms of its occurrence and progression and search for novel targets for diagnosis and treatment is urgently needed (Alberts 2020). The regulatory role of micro-ribonucleic acids (miRNAs) is found in inflammatory responses, and they also participate in the pathophysiological process of IS (Mancha et al. 2020). As reported, upregulating miR-124 is able to reduce ischemic infarct area and promote neurological function recovery (Huang et al. 2019). Mammalian target of rapamycin (mTOR) is a non-classical type of serine/threonine protein kinase, and IS-induced brain injury is also associated with mTOR signaling pathway (Zhang et al. 2020b). MiR-182, which destroys the blood-brain barrier integrity through suppressing the mTOR/FOXO1 pathway, is regarded as a latent treatment target for IS (Zhang et al. 2020a). MiR-155, positioned at chromosome 21, the third exon of a non-coding transcript from the B-cell integration cluster (BIC), participates in the onset and development of IS (Yang et al. 2021). According to the report of Pena-Philippides et al. (2018), miR-155 expression level rose dramatically in the brain tissues of IS rats, further indicating the relation between miR-155 and pathogenesis of IS (Xing et al. 2016). At present, the specific function of miR-155 in the case of IS and its mechanism remain elusive.

Objectives

Therefore, the purpose of this study was to detect the serum expression level of miR-155 in IS patients and healthy individuals and to determine miR-155 and mTOR levels in BV2 cells after induction of OGD, thus investigating the performance of the miR-155/mTOR pathway in the developing process of IS.

MATERIAL AND METHODS

Total RNA Extraction from Serum of IS Patients

Thirty patients with IS admitted to the researchers' hospital from June 2020 to June 2021 were en-

*Address for correspondence:
Zhuquan Hong
E-mail: hongzqqfh@peak-edu.cn

rolled as subjects, while 30 healthy controls in the same period were selected. Approval for this study protocol was obtained from the Ethics Committee of the researchers' hospital. In situations where participants and their families were informed of research content, they signed the informed consent document. About 3.5 mL of fasting venous blood was extracted from each participant and placed in an anticoagulant tube, from which the supernatant was collected by means of 8 min centrifugation (3,000 rpm and 4°C).

NIHSS Scoring of IS Patients

The evaluation of neurological deficits in patients with IS was implemented based on the National Institute of Health Stroke Scale (NIHSS) at 1, 7 and 14 days after onset, including consciousness level, visual acuity and visual field, eye movement, facial muscle activity, upper- and lower-extremity movement abilities and cerebellar control of balance.

Incubation of BV2 and HMC3 Cells

Mouse microglial BV2 and HMC3 cells offered by ATCC (USA) were incubated in complete Dulbecco's Modified Eagle's Medium (DMEM) (HyClone) containing fetal bovine serum (FBS) (10 percent) which was mixed with penicillin (100 U/mL) and streptomycin (100 μg/mL), followed by cultivation in an incubator under 5 percent CO_2 at 37°C.

Cell OGD Modeling

BV2 and HMC3 cells (logarithmic growth phase) were implanted into a 6-well plate (100,000 cells/well). After PBS rinsing of the cells in experimental group twice, the culture medium was substituted by glucose-free MEM supplemented with 10 percent FBS. Subsequently, the 6-well plate was incubated for 4 h in a tri-gas incubator with an atmosphere of 5 percent CO_2, 95 percent N_2 and 37°C, so as to establish an oxygen-glucose deprivation (OGD) model.

Cell Transfection

MiR-155-mimic, miR-155-inhibitor, mimic-negative control (NC) and inhibitor-NC were provided by Shanghai GenePharma Co., Ltd. BV2 and HMC3 cells (5×10^6 cells/well) were seeded into a 6-well plate. Then Lipofectamine 2000 (5 μl, Invitrogen, USA) and miR-155-mimic/mimic-NC or miR-155-inhibitor/inhibitor-NC (100 pM) were diluted using 125 μl of antibiotics-free Opti-MEM to prepare solutions A and B, respectively. Subsequent to 5 min of standing, solution A was fully mixed with solution B and incubated at 37°C. After 15 min, BV2 and HMC3 cells in experimental group were incubated in 200 μL of the obtained mixture for 6 h, followed by further cultivation in a complete culture medium for 48 h, while those in control group were incubated routinely. Total RNA was extracted after 48 h, and cellular protein was extracted after 72 h. Finally, qRT-PCR and Western blotting were performed to verify the knockout and overexpression efficiency of miR-155, respectively.

Cell Counting Kit-8 (CCK-8) Assay

After the above treatment, BV2 and HMC3 cells were inoculated into a 96-well plate, with 1.5×10^3 cells/well as the density. Thereafter, each well was added with CCK-8 solution (10 μL, Beyotime Biotechnology, China) at 0, 4, 8, 12 and 24 h. Following 2 h of 37°C incubation, a microplate reader (FlexStation III ROM, USA) was employed to determine the optical density (OD) at 450 nm wavelength.

Quantitative Reverse Transcription-Polymerase Chain Reaction (qRT-PCR)

With the addition of TRIzol reagent (1 mL in total, Invitrogen, USA) into serum and cell samples, total RNA was extracted, and the RNA concentration was determined. Then the total RNA (500 ng) was subjected to reverse transcription into cDNA complying with the PrimeScript™ RT reagent Kit (TaKaRa, Japan) instructions, which was amplified by PCR using qPCR system (Bio-Rad, USA) with qRT-PCR kits (Nanjing Vazyme Biotech Co., Ltd.). All primers were bought from Sangon Biotech (Shanghai) Co., Ltd., configured with the following primer sequences: miR-155: F: 5'-AACATTCATTGCTGTCGGTGGG-3' and R: 5'-GCGAGCACAGAATTAATACGACTCAC-3', mTOR: F: 5'-ATGCTTGGAACCGGACCTG-3' and R: 5'-TCTTGACTCATCTCTCGGAGTT-3', and U6: F: 5'-CTCGCATCGCGTAAGGCACA-3' and R: 5'-AACGCTACTCGAATTAGCGT-3'. U6 was uti-

lized as the internal reference for normalization of the levels of miR-155 and mTOR. Finally, $2^{-\Delta\Delta Ct}$ method was adopted to calculate the relative expression levels.

Western Blotting

Cell lysis was exerted on ice using RIPA lysis buffer (CST, USA), which lasted for 30 min. Then the protein supernatant was collected after the cells were centrifuged (12,000 g and 4°C) for 10 min. The protein concentration was quantified by virtue of BCA kit (Beyotime Biotechnology, Shanghai). Next, the protein was subjected to separation *via* 10 percent sodium dodecyl sulfate-polyacrylamide gel electrophoresis as well as electrotransfer onto a PVDF membrane (0.45 μm, Millipore, USA). After that, 1.5 h of membrane sealing (37°C) with 5 percent skimmed milk powder and overnight membrane incubation (4°C) with primary antibodies against mTOR and GAPDH were conducted. Later, following washing with TBST for 3×10 min, 1-2 h of membrane incubation with horseradish peroxidase (HRP)-labeled secondary antibodies was carried out at room temperature. After being washed in TBST again for three times, the membrane received color development using ECL system (Wuhan Boster Biological Technology Co., Ltd). Finally, ChemiDoc XRS + Imaging System (Bio-Rad, USA) was utilized to scan the protein bands. All the antibodies mentioned above were purchased from CST (USA).

Statistical Analysis

GraphPad software was employed to accomplish statistical analysis. The experimental data were presented as mean ± standard deviation. The comparison between two groups was realized through student's *t*-test. For all the tests set as two-tailed, P<0.05 meant that the difference was statistically significant.

RESULTS

Significant Up-regulation of Serum miR-155 Expression in IS Patients

The expression levels of serum miR-155 in IS patients (n=30) as well as healthy controls (n=30) were examined through qRT-PCR. It was manifested that miR-155 expression level rose notably in serum of IS patients ((4.213 ± 0.321) vs. (1.823 ± 0.232), P<0.001) (Fig. 1).

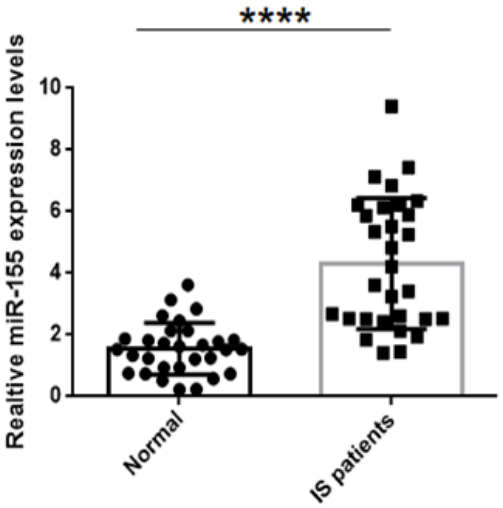

Fig. 1. Significant up-regulation of miR-155 expression in serum of patients with IS measured by qRT-PCR ****P<0.001 vs. healthy controls

NIHSS Scores of Patients Presenting Different Expression Levels of miR-155 as IS Progressed

At 1, 7 and 14 days, neurological deficits in patients were evaluated by the NIHSS, and the results displayed that the NIHSS score of patients declined progressively after the onset of IS. In light of qRT-PCR results, patients were assigned to high miR-155 expression group and low miR-155 expression group with 50 percent as the dividing line (Table 1). There was a clearly lower NIHSS score ((4.523 ± 0.121), (3.323 ± 0.212) and (2.692 ± 0.302) points) in low miR-155 expression group than that in high miR-155 expression group ((7.732 ± 0.173), (6.821 ± 0.283) and (6.872 ± 0.327) points) on the 1st, 7th and 14th days after onset (***P<0.005, ****P<0.001) (Fig. 2).

Table 1: Proportions of patients with different miR-155 expression levels in IS patients on the 1st, 7th and 14th days

Proportion	*Day 1*	*Day 7*	*Day 14*
High miR-155 expression	50%	50%	50%
Low miR-155 expression	50%	50%	50%

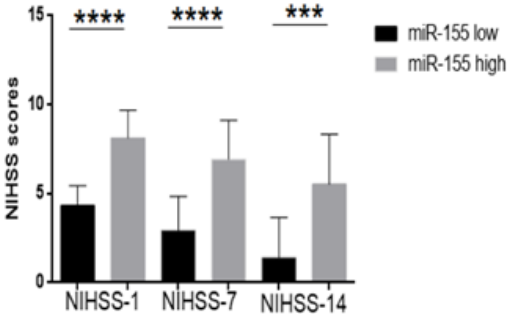

Fig. 2. NIHSS scores of patients with different expression levels of miR-155 on the 1st, 7th and 14th days after onset
*****P<0.001 and ****P<0.0005 vs. low miR-155 expression group**

Expressions of miR-155 and mTOR Protein in BV2 and HMC3 Cells after OGD Treatment

According to the results of RT-PCR, the relative expression of miR-155 in BV2 cells after OGD treatment was (8.523 ± 0.098), while that of control group was (1.782 ± 0.023) (Fig. 3A). In contrast with control group, OGD-treated BV2 cells displayed significantly increased miR-155 expression (P<0.05). Furthermore, it was indicated by Western blotting that the relative expression of mTOR protein in BV2 cells after OGD treatment was (0.423 ± 0.102), while that of control group was (0.982 ± 0.162) (Fig. 3B and C). The expression of mTOR protein was overtly lower in OGD-treated BV2 cells than that in control group (P<0.05).

Similarly, RT-PCR exhibited that the relative miR-155 expression was (11.892 ± 0.105) in HMC3 cells after OGD treatment, while that in control group was (1.913 ± 0.021) (Fig. 3A). The expression of miR-155 significantly increased in OGD-treated HMC3 cells in comparison with that in control group (P<0.05). As shown in Western blotting results, the relative expression of mTOR protein in HMC3 cells after OGD treatment was (0.561± 0.123), while that of control group was (1.529 ± 0.142) (Fig. 3B and C). In contrast, OGD-treated HMC3 cells had apparently lower mTOR protein expression than control group (P<0.05).

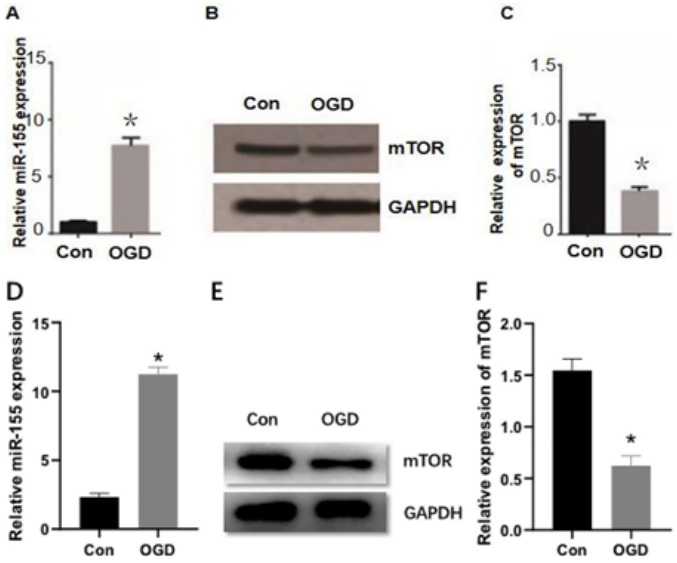

Fig. 3. Expressions of miR-155 and mTOR protein in BV2 and HMC3 cells after OGD treatment. A: Detection of miR-155 expression in OGD-treated BV2 cells by qRT-PCR; B and C: determination of mTOR protein expression in OGD-treated BV2 cells by Western blotting; D: detection of miR-155 expression in OGD-treated HMC3 cells by qRT-PCR; E and F: determination of mTOR protein expression in OGD-treated HMC3 cells by Western blotting
***P<0.05 *vs.* control group**

Influence of miR-155 on OGD-treated BV2 and HMC3 Cell Proliferation

Based on CCK-8 assay results, the survival rate of OGD-treated BV2 and HMC3 cells was significantly reduced compared with that of control group (P<0.001). The survival rate of BV2 and HMC3 cells after miR-155-mimic transfection plus OGD treatment declined remarkably in comparison with that of OGD-treated cells with or without mimic-NC transfection (P<0.001). Besides, the survival rate of BV2 and HMC3 cells receiving miR-155-inhibitor transfection plus OGD treatment was raised compared with that of OGD-treated cells subjected to inhibitor-NC transfection or not, but it remained low in contrast with that of control group (P<0.001) (Fig. 4). The OD values of BV2 and HMC3 cells are listed in Tables 2 and 3.

Influence of miR-155 on OGD-treated BV2 and HMC3 Cell Apoptosis

Flow cytometry exhibited that for control group, OGD-treated group, transfected mimic-NC plus OGD-treated group and miR-155 mimic plus OGD-treated group, the early apoptosis rates of BV2

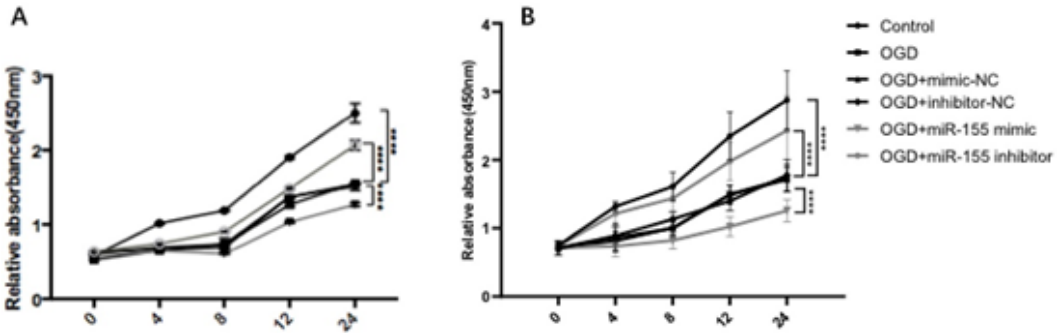

Fig. 4. Influence of miR-155 on OGD-treated BV2 and HMC3 cell proliferation. Measurement of survival rates of cells subjected to OGD treatment, transfection with mimic-NC plus OGD treatment, transfection with miR-155-mimic plus OGD treatment, transfection with inhibitor-NC plus OGD treatment, and transfection with miR-155-inhibitor plus OGD treatment by CCK-8 assay
******P<0.001**

Table 2: OD values of BV2 cells treated for 0, 4, 8, 12 and 24 h

Groups	*0 h*	*4 h*	*8 h*	*12 h*	*24 h*
Control	0.682±0.078	1.124±0.066	1.322±0.234	1.922±0.237	2.524±0.283
OGD	0.629±0.152	0.798±0.324	0.902±0.029	1.434±0.022	1.693±0.096
OGD+mimic-NC	0.601±0.017	0.712±0.035	0.898±0 .154	1.422±0.207	1.634±0.026
OGD+miR-155 mimic	0.602±0.127	0.721±0.081	0.701±0.122	0.813±0.092	1.212±0.023
OGD+inhibitor-NC	0.642±0.217	0.754±0.026	0.878±0.254	1.352±0.107	1.525±0.046
OGD+miR-155 inhibitor	0.673±0.082	0.792±0.026	0.923±0.044	1.562±0.037	1.894±0.036

Table 3: OD values of HMC3 cells treated for 0, 4, 8, 12 and 24 h

Groups	*0 h*	*4 h*	*8 h*	*12 h*	*24 h*
Control	0.747±0.067	1.317±0.071	1.611±0.213	2.347±0.353	2.876±0.431
OGD	0.703±0.094	0.865±0.214	0.998±0.121	1.489±0.136	1.712±0.177
OGD+mimic-NC	0.712±0.103	0.812±0.141	1.004±0 .097	1.496±0.129	1.733±0.201
OGD+miR-155 mimic	0.711±0.104	0.734±0.156	0.821±0.125	1.022±0.147	1.256±0.159
OGD+inhibitor-NC	0.642±0.217	0.754±0.026	0.878±0.254	1.352±0.107	1.525±0.046
OGD+miR-155 inhibitor	0.673±0.082	0.792±0.026	0.923±0.044	1.562±0.037	1.894±0.036

cells were 1.18, 22.09, 22.78 and 7.30 percent, respectively, and the late apoptosis rates were 1.31, 14.77, 11.02 and 2.08 percent, respectively. The early apoptosis rates HMC3 cells were 9.71, 29.13, 25.66 and 19.81 percent, respectively, and the late apoptosis rates were 1.14, 7.21, 5.74 and 2.96 percent, respectively. Clearly, both the early and late apoptosis rates of BV2 and HMC3 cells after OGD treatment were elevated in contrast to those of control group ($P<0.05$). Additionally, in comparison to OGD with or without transfection of mimic-NC group, miR-155 mimic plus OGD-treated group had further increased early and late apoptosis rates of BV2 and HMC3 cells ($P<0.05$) (Fig. 5).

MiR-155 and mTOR Expressions After miR-155-mimic Transfection

Following transfection of BV2 cells with miR-155-mimic, the relative miR-155 expression levels were (1.522±0.187), (1.454±0.086) and (7.678±1.254), respectively, in blank group, NC group and transfection group, with statistically significant differences between blank and NC groups and transfection group ($P<0.05$), suggesting that the successful transfection facilitated miR-155 expression in BV2 cells (Fig. 6A). Given transfection with miR-155-mimic, BV2 cells displayed the relative expression levels of mTOR mRNA at (1.423±0.248), (1.389±0.113) and (0.289±0.051), and the relative expression levels of mTOR protein were (1.487±0.232), (1.432±0.156) and (0.276±0.076), respectively, in blank group, NC group and transfection group. The differences in mRNA and protein expression levels of mTOR between transfection group and blank and NC groups were of statistical significance ($P<0.05$), indicating the inhibitory effect of miR-155-mimic transfection on the expressions of mTOR mRNA and protein in BV2 cells (Fig. 6B-D).

The relative miR-155 expression levels in HMC3 cells subjected to miR-155-mimic transfection were (2.012±0.047), (1.989 ± 0.016) and (11.231 ±0.339), respectively, in blank group, NC group and transfection group, where blank and NC groups were statistically significant different from transfection group ($P<0.05$), indicating that the successful transfection facilitated miR-155 expression in HMC3 cells (Fig. 6E). In HMC3 cells with miR-155-mimic transfected, the relative expression levels of mTOR mRNA were (1.583 ± 0.324), (1.592 ±0.293) and (0.273 ± 0.194), and the relative expression levels of mTOR

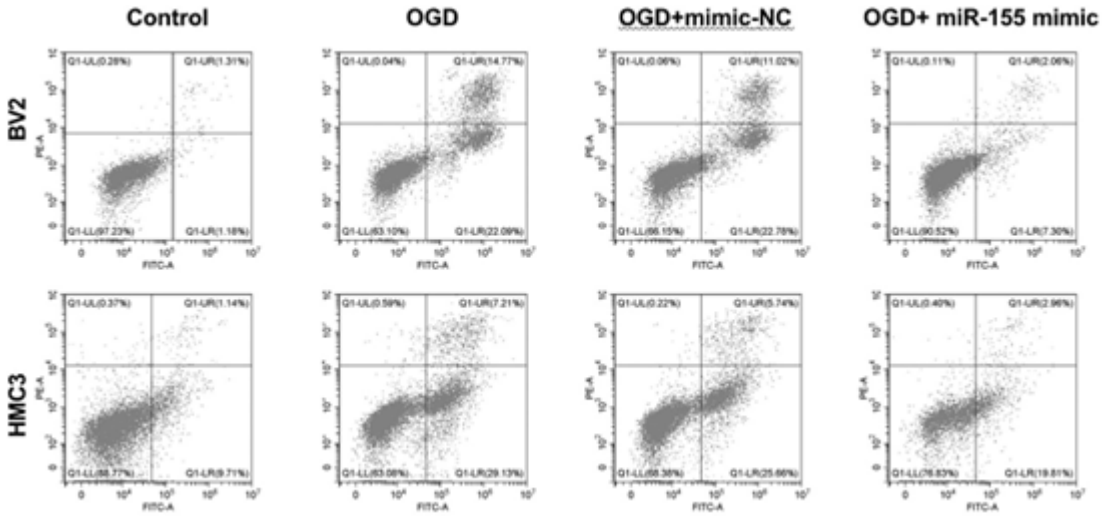

Fig. 5. Influence of miR-155 on OGD-treated BV2 and HMC3 cell apoptosis. Measurement of apoptotic rates of cells subjected to OGD treatment, transfection with mimic-NC plus OGD treatment, transfection with miR-155-mimic plus OGD treatment, transfection with inhibitor-NC plus OGD treatment, and transfection with miR-155-inhibitor plus OGD treatment by flow cytometry

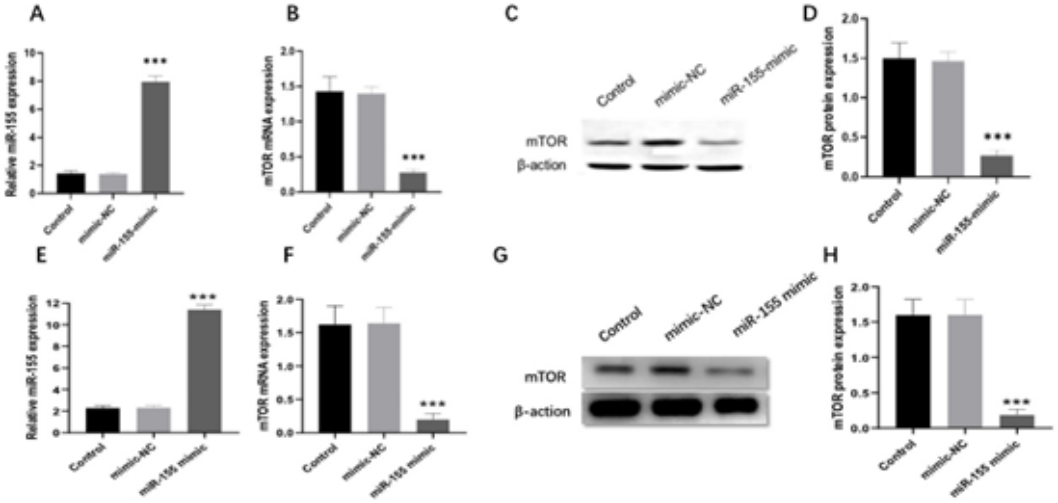

Fig. 6. Expressions of miR-155 and mTOR in BV2 and HMC3 cells after transfection with miR-155-mimic. A: Expression of miR-155 in BV2 cells transfected with miR-155-mimic; B: expression of mTOR mRNA in BV2 cells transfected with miR-155-mimic; C and D: expression of mTOR protein in BV2 cells transfected with miR-155-mimic; E: expression of miR-155 in HMC3 cells transfected with miR-155-mimic; F: expression of mTOR mRNA in HMC3 cells transfected with miR-155-mimic; G and H: expression of mTOR protein in HMC3 cells transfected with miR-155-mimic

protein were (1.512 ± 0.151), (1.494± 0.123) and (0.269 ± 0.092), respectively, in blank group, NC group and transfection group. In other words, the mRNA and protein expression levels of mTOR displayed statistically significant differences between blank and NC groups and transfection group (P<0.05), suggesting that in HMC3 cells, miR-155-mimic transfection suppressed mTOR mRNA and protein expressions (Fig. 6F-H).

Expressions of miR-155 and mTOR Following Transfection of miR-155-inhibitor

In BV2 cells, the relative expression levels of miR-155 subsequent to miR-155-inhibitor transfection were (1.465±0.217), (1.445±0.126) and (0.178±0.078), respectively, in blank group, NC group and transfection group. The differences were of statistical significance between transfection group and blank and NC groups (P<0.05), confirming that the successful transfection of BV2 cells suppressed miR-155 expression (Fig. 7A). Furthermore, the relative expression levels of mTOR mRNA were (1.634±0.248), (1.567±0.121) and (8.589±0.651), and the relative expression levels of mTOR protein were (1.723±0.212), (1.611±0.096) and (8.434±0.676), respectively, in blank group, NC group and transfection group. The differences in mTOR mRNA and protein expressions between transfection group and blank and NC groups were of statistical significance (P<0.05), revealing that for BV2 cells, miR-155-inhibitor transfection promoted mTOR mRNA and protein expressions (Fig. 7B-D).

Regarding HMC3 cells with miR-155-inhibitor transfected, the relative miR-155 expression levels were (2.214±0.302), (2.019 ± 0.259) and (0.195 ± 0.083), respectively, in blank group, NC group and transfection group. The differences were of statistical significance between transfection group and blank and NC groups (P<0.05), demonstrating that the successful transfection inhibited the miR-155 expression in HMC3 cells (Fig. 7E). The relative expression levels of mTOR mRNA were (1.921 ± 0.082), (1.829 ±0.074) and (11.532 ± 0.293), and the relative expression levels of mTOR protein were (1.839 ± 0.028), (1.812 ± 0.023) and (10.539 ± 0.029), respectively, in blank group, NC group and transfection group. The expression levels of mTOR mRNA and protein presented to be different between blank and NC groups and transfection group, which was statistically significant (P<0.05), revealing that the transfection of HMC3 cells with

miR-155-inhibitor faciliateded mTOR mRNA and protein expressions (Fig. 7F-H).

DISCUSSION

IS ranks forefront in mortality and disability worldwide. Thrombosis or other emboli, blocking the blood supply to the brain, may lead to hypoxia-ischemia injury in central nervous cells, thus inducing notable disorders of glucose metabolism and ion gradient within a few minutes. As a result, cell depolarization and imbalance of exchange between intra- and extra-cellular ions occur, causing cell apoptosis and permanent necrosis in the center of ischemic focus (Abdel-Magid 2017). Relations exist between IS and multiple factors, involving cellular bioenergy exhaustion, oxidative stress, excitotoxicity, dysfunction of the blood-brain barrier, post-ischemic inflammation, microvascular damage as well as intracranial atherosclerosis (AS) (Ajoolabady et al. 2021; Qiu et al. 2021). At present, the pathogenesis and prognostic influencing factors of IS remain elusive. Consequently, further investigating the IS mechanism at the molecular level may be remarkably beneficial for the early clinical diagnosis of IS and exploration of potential targets for drug treatment. Being a category of non-coding endogenous small RNA molecules, miRNAs, with 20-22 nucleotides in length, can suppress and degrade target mRNAs by means of direct conjugation with their 3'-untranslated region (3'-UTR), thus reducing the expression of target protein (Kota and Kota 2017). As corroborated by a previous study, injection of miR-155 inhibitor *via* tail vein can target Rheb protein to enhance the stability of capillary endothelial zonula occludens-1 (ZO-1), prominently lowering the infarct area of rats with distal middle cerebral artery occlusion (dMCAO) (34%) (Caballero-Garrido et al. 2015). MiR-155 also plays certain roles in amyotrophic lateral sclerosis (ALS), epilepsy, experimental autoimmune encephalomyelitis (EAE), spinal cord injury, Alzheimer's disease (AD), multiple sclerosis (MS), Parkinson's disease (PD), brain tumors,

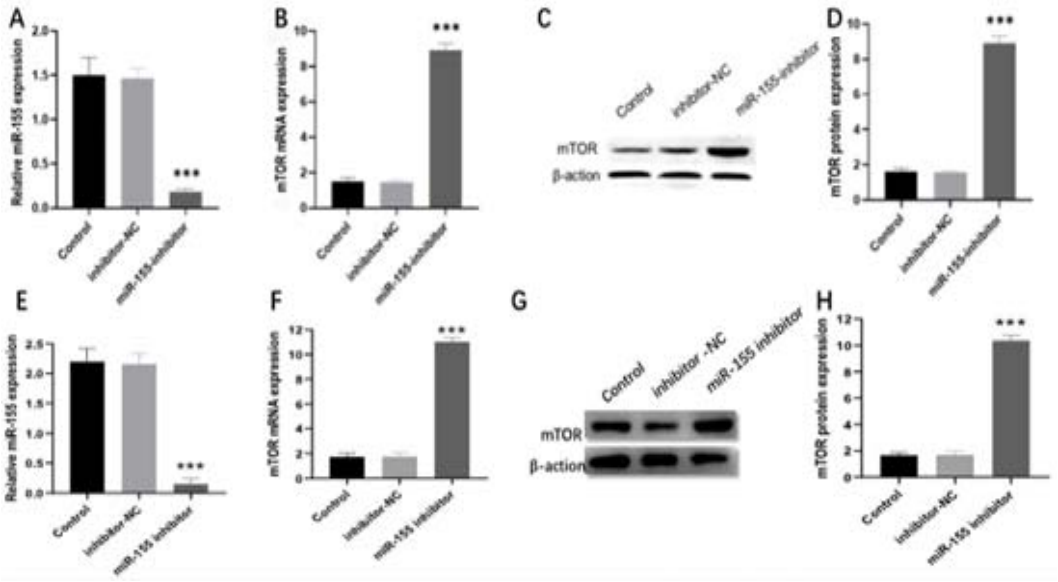

Fig. 7. Expressions of miR-155 and mTOR in BV2 and HMC3 cells after transfection with miR-155-inhibitor. A: Expression of miR-155 in BV2 cells transfected with miR-155-inhibitor; B: expression of mTOR mRNA in BV2 cells transfected with miR-155-inhibitor; C and D: determination of mTOR protein expression in BV2 cells transfected with miR-155-inhibitor by Western blotting; E: expression of miR-155 in HMC3 cells transfected with miR-155-inhibitor; F: expression of mTOR mRNA in HMC3 cells transfected with miR-155-inhibitor; G and H: determination of mTOR protein expression in HMC3 cells transfected with miR-155-inhibitor by Western blotting

and so on, as numerous studies reported. Nevertheless, the specific mechanism of miR-155 in IS still needs to be elucidated.

Despite the fact that there are only a few hundreds of miRNAs, which are defined as a class of small RNA molecules with high conservation, each of them is considered to possibly regulate hundreds of target genes. MiRNAs may exert regulatory effects in over one-third human genes. Furthermore, miRNAs are able to greatly modulate gene expression at post-transcriptional level in various tissues such as brain thus affecting cell development, proliferation, differentiation as well as apoptosis (Ludwig et al. 2016). Several miRNAs have recently been distinguished to be capable of participating and regulating multiple signal pathways related to stroke progression and recovery, including nerve regeneration, morphological alteration of endothelial cells and neuroinflammation (Gaudet et al. 2018). MiR-155, a multi-functional miRNA, is found to modulate varieties of physiological and pathological processes, including immunity, differentiation of hematopoietic lineage, inflammation, cardiovascular diseases and cancers. Besides, miR-155 can regulate vascular endothelial function, repress inflammatory response and promote cell regeneration, thus restoring blood supply in the peri-infarct zone and facilitating neurological function recovery (O'Connell et al. 2010). In brain of IS rats, miR-155 more than 1.5 times lower than that found in normal rats may be a potential biomarker of brain injury (Liu et al. 2010). Specifically restraining miR-155 expression may not only induce the generation of endothelial nitric oxide synthase (eNOS) together with nitric oxide (NO), but also mitigate vascular inflammation, while miR-155 overexpression is able to trigger morphological alteration of endothelial cells and impede endothelial cell migration (Weber et al. 2014). In a previous trial, mice were intravenously injected with a specific inhibitor of miR-155 at 48 h subsequent to dMCAO, and then the microvascular system in peri-infarct zone, the area of infarct and the recovery of function were evaluated 1, 2 and 3 weeks later. The results manifested the blood flow recovery and improvement of microvascular integrity in the peri-infarct zone of mice and alleviated brain tissue damage, revealing that suppressing the *in vivo* miR-155 expression is conducive to modulating angiogenesis and promoting functional recovery after IS (Caballero-Garrido et al. 2015).

Though this study, the serum miR-155 expression level was notably elevated in patients with IS in contrast with that in healthy individuals. Zhang and Guo (2021) reported the down-regulation of serum miR-155 in patients suffering from coronary heart disease, and argued that miR-155 probably served as a novel promising biomarker for assisting coronary heart disease diagnosis and an independent predictor of severe multiple stenosis and reduced blood supply range of coronary artery. In addition, hypertension also has an influence on miR-155 expression level, while its specific expression can be found in AS (Nazari-Jahantigh et al. 2012; Huang et al. 2016). As previous and current research reported, miR-155 is a promising diagnostic marker for IS. NIHSS score is primarily used to evaluate neurological deficits in patients with IS and predict their prognosis, which contributes to formulating individualized therapeutic regimens. In this study, IS patients were assigned to high miR-155 expression group and low miR-155 expression group. Through analysis about NIHSS scores of patients on the 1st, 7th and 14th days after the onset of IS, it could be seen that miR-155 expression level declined progressively, and NIHSS score in high miR-155 expression group remained consistently raised in comparison to that in low miR-155 expression group. The findings denoted that miR-155 may represent a biological marker for predicting the prognosis of IS, while the higher the miR-155 expression, the poorer the prognosis. mTOR, which can regulate protein synthesis and autophagy, is considered to be a target extensively applied in immunotherapy. Normally, mTOR is activated by virtue of sufficient nutrients plus oxygen, thereby stimulating anabolic processes (that is, protein synthesis) and suppressing catabolic processes (that is, autophagy). However, nutrient supply is reduced after onset of IS, which will limit mTOR activation, thus inhibiting protein synthesis and inducing autophagy. Rapamycin as an mTOR inhibitor is capable of reducing the expression of MMP-9 in IS mice, elevating eNOS activity, ameliorating residual cerebral blood flow (CBF) in mouse model of Alzheimer's disease (AD), and facilitating cerebrovascular integrity and functional recovery (Lin et al. 2013; Su et al. 2014). In a trial carried out in mouse models of AS and vascular cognitive impairment with deficiency of low-density lipoprotein receptor, CBF and cerebrovascular density are restored by rapamycin, which exerts

greater neuroprotection (Jahrling et al. 2018). In this study, OGD environment of nerve cells *in vitro* was simulated by OGD modeling in BV2 cells. The findings displayed that BV2 cells in OGD group presented a prominently higher miR-155 expression level than those in normal group. Based on Western blotting results, BV2 cells of OGD group exhibited markedly decreased protein expression of mTOR, indicating that miR-155 and mTOR protein participated in the regulatory mechanism of OGD-treated BV2 cells. It was demonstrated by the findings of cell viability assay that OGD-treated cells displayed an evidently reduced survival rate, while a further reduction was observed in cells subjected to miR-155-mimic transfection and OGD treatment ($P<0.001$). The transfection with miR-155-inhibitor plus OGD treatment resulted in a higher cells survival rate in contrast to that in OGD group, but it was still low compared with that in control group ($P<0.001$), suggesting that highly expressed miR-155 suppresses neuron viability while inhibiting miR-155 contributes to the recovery of neuron viability after OGD-induced stress. In addition, after transfection of BV2 cells using miR-155 mimic or inhibitor, the elevated expression of miR-155 would repress mTOR transcription and translation, whereas the downregulation of miR-155 facilitated mTOR mRNA and protein expressions.

CONCLUSION

In conclusion, miR-155 increases in the pathogenetic process of IS and is negatively correlated with the prognosis of IS patients. Moreover, miR-155 is capable of repressing cell viability and mTOR protein expression in mouse microglial BV2 cells and facilitating OGD-induced stress response.

RECOMMENDATIONS

MiR-155 is a potential important diagnostic and prognostic indicator and therapeutic target for IS, which should be validated by further clinical studies.

FUNDING

This research is funded by Startup Fund for scientific research, Fujian Medical University (Grant number: 2020QH1262.)

REFERENCES

Abdel-Magid AF 2017. Selective Estrogen Receptor Degraders (SERDs): A promising treatment to overcome resistance to endocrine therapy in ERα-positive breast cancer. *ACS Med Chem Lett*, 8: 1129-1131.

Ajoolabady A, Wang S, Kroemer G et al. 2021. Targeting autophagy in ischemic stroke: From molecular mechanisms to clinical therapeutics. *Pharmacol Ther*, 225: 107848.

Alberts MJ 2020. In ischemic stroke, thrombectomy alone was noninferior to thrombectomy plus alteplase for functional outcome at 90 days. *Ann Intern Med*, 173: Jc31.

Caballero-Garrido E, Pena-Philippides JC, Lordkipanidze T et al. 2015. In vivo inhibition of mir-155 promotes recovery after experimental mouse stroke. *J Neurosci*, 35: 12446-12464.

Charbonnier G, Bonnet L, Biondi A et al. 2020. Intracranial bleeding after reperfusion therapy in acute ischemic stroke. *Front Neurol*, 11: 629920.

Feigin VL, Nguyen G, Cercy K et al. 2018. Global, regional, and country-specific lifetime risks of stroke, 1990 and 2016. *New Engl J Med*, 379: 2429-2437.

Gaudet AD, Fonken LK, Watkins LR et al. 2018. MicroRNAs: Roles in regulating neuroinflammation. *Neuroscientist*, 24: 221-245.

Gervois P, Lambrichts I 2019. The emerging role of triggering receptor expressed on myeloid cells 2 as a target for immunomodulation in ischemic stroke. *Front Immunol*, 10: 1668.

Huang WY, Jiang C, Ye HB et al. 2019. miR-124 upregulates astrocytic glutamate transporter-1 via the Akt and mTOR signaling pathway post ischemic stroke. *Brain Res Bull*, 149: 231-239.

Huang Y, Chen J, Zhou Y et al. 2016. Circulating miR155 expression level is positive with blood pressure parameters: Potential markers of target-organ damage. *Clin Exp Hypertens*, 38: 331-336.

Jahrling JB, Lin AL, DeRosa N et al. 2018. mTOR drives cerebral blood flow and memory deficits in LDLR(-/-) mice modeling atherosclerosis and vascular cognitive impairment. *J Cereb Blood Flow Metab*, 38: 58-74.

Kota SK, Kota SB 2017. Noncoding RNA and epigenetic gene regulation in renal diseases. *Drug Discov Today*, 22: 1112-1122.

Lin AL, Zheng W, Halloran JJ et al. 2013. Chronic rapamycin restores brain vascular integrity and function through NO synthase activation and improves memory in symptomatic mice modeling Alzheimer's disease. *J Cereb Blood Flow Metab*, 33: 1412-1421.

Liu DZ, Tian Y, Ander BP et al. 2010. Brain and blood microRNA expression profiling of ischemic stroke, intracerebral hemorrhage, and kainate seizures. *J Cereb Blood Flow Metab*, 30: 92-101.

Ludwig N, Leidinger P, Becker K et al. 2016. Distribution of miRNA expression across human tissues. *Nucl Acids Res*, 44: 3865-3877.

Mancha F, Escudero-Martinez I, Zapata-Arriaza E et al. 2020. Circulating microRNA after autologous bone marrow mononuclear cell (BM-MNC) injection in patients with ischemic stroke. *J Invest Med*, 68: 807-810.

Nazari-Jahantigh M, Wei Y, Noels H et al. 2012. MicroRNA-155 promotes atherosclerosis by repressing Bcl6 in

macrophages. *J Clin Invest*, 122: 4190-4202.
O'Connell RM, Kahn D, Gibson WS et al. 2010. MicroRNA-155 promotes autoimmune inflammation by enhancing inflammatory T cell development. *Immunity*, 33: 607-619.
Pena-Philippides JC, Gardiner AS, Caballero-Garrido E et al. 2018. Inhibition of MicroRNA-155 supports endothelial tight junction integrity following oxygen-glucose deprivation. *J Am Heart Assoc*, 7: e009244.
Qiu YM, Zhang CL, Chen AQ et al. 2021. Immune cells in the BBB disruption after acute ischemic stroke: Targets for immune therapy? *Front Immunol*, 12: 678744.
Su J, Zhang T, Wang K et al. 2014. Autophagy activation contributes to the neuroprotection of remote ischemic perconditioning against focal cerebral ischemia in rats. *Neurochem Res*, 39: 2068-2077.
Weber M, Kim S, Patterson N et al. 2014. MiRNA-155 targets myosin light chain kinase and modulates actin cytoskeleton organization in endothelial cells. *Am J Physiol -Heart Circ Physiol*, 306: H1192-1203.
Xing G, Luo Z, Zhong C et al. 2016. Influence of miR-155 on cell apoptosis in rats with ischemic stroke: Role of the Ras Homolog Enriched in Brain (Rheb)/mTOR Pathway. *Med Sci Monit*, 22: 5141-5153.
Yang J, Zhu X, Hu H et al. 2021. The inhibitory effect of Gualou Guizhi Decoction on post-ischemic neuroinflammation via miR-155 in MCAO rats. *Ann Palliat Med*, 10: 1370-1379.
Zhang R, Guo HP 2021. Correlation between abnormal expression of Mir-126 and Mir-155 in serum and degree of coronary artery disease in patients with coronary heart disease. *J Qiqihar Med Coll*, 42: 1473-1479.
Zhang T, Tian C, Wu J et al. 2020a. MicroRNA-182 exacerbates blood-brain barrier (BBB) disruption by downregulating the mTOR/FOXO1 pathway in cerebral ischemia. *FASEB J*, 34: 13762-13775.
Zhang Y, He Q, Yang M et al. 2020b. Dichloromethane extraction from Piper nigrum L. and P. longum L. to mitigate ischemic stroke by activating the AKT/mTOR signaling pathway to suppress autophagy. *Brain Res*, 1749: 147047.

Paper received for publication in
Paper accepted for publication in